*Journal of Ceramic Processing Research. Vol. 13, No. 3, pp. 221~225 (2012)*

J O U R N A L O F
**Ceramic Processing Research**

# Rapid synthesis of hydroxyapatite nanopowders by a microwave-assisted combustion method

**Nagmeh Bovand[a], Sousan Rasouli[b,*], Mohammad-Reza Mohammadi[c] and Davood Bovand[d]**

[a]*Department of Biomedical Engineering, Biomaterials Science and Research, Islamic Azad University, Tehran- Iran*
[b]*Department of Nanomaterials & Nanocoatings, Institute for Color Science and Technology, 55 Vafamanesh Ave., HosseinAbad Square, Pasdaran St, 1668814811, Tehran-Iran*
[c]*Sharif University of Technology, Tehran-Iran*
[d]*Department of Materials Science, Semnan University, Semnan-Iran*

**Nano bioactive hydroxyapatite ($Ca_{10}(PO_4)_6(OH)_2$, HAp) ceramic powders have been synthesized by a microwave-assisted combustion method. The powders were synthesized using calcium nitrate tetrahydrate (as the source of calcium) and sodium phosphate dibasic anhydrous (as the source of phosphate ions). Glycine, citric acid and urea were used as fuesl. The influence of the fuel type on the structure and morphology of the samples was studied. Results by X-ray diffraction and Fourier-transform infrared spectroscopy showed the formation of hydroxyapatite as a major phase for all the samples. Using the Scherrer formula, the average crystallite size was found to be in the range of 10 to 28 nm. SEM-EDX results showed highly crystalline nano-powders with an elemental composition of Ca and P in the HAp phase. The morphology of the particles was dependent an the fuel type and changed from semi-spherical to elongated. Smaller particles were obtained with glycine as the fuel.**

**Key words: Hydroxyapatite, Combustion synthesis, Fuel, Morphology.**

## Introduction

Bioceramic materials are widely used to repair and reconstruct damaged parts of the human skeleton especially as bone substitutes in the filling of bone defects [1].

Major phases of calcium phosphate to be found are hydroxyapatite [$Ca_{10}(PO_4)_6(OH)_2$], octacalcium phosphate [OCP, $Ca_8H_2(PO_4)_6$], tricalcium phosphate [TCP, $Ca_3(PO_4)_2$], dicalcium phosphate dehydrate [DPCD, $CaHPO_4$. $2H_2O$] and dicalcium phosphate [DCP, $Ca_2P_2O_7$] [2].

HAp is a preferred material for bone repair because of its stability under in vivo conditions, compositional similarity, excellent biocompatibility, osteoconductivity, and ability to promote osteoblasts functions [3]. HAp elicits specific biological responses at the interface, which results in the formation of a strong bond between the bone tissues and the material [4]. Its various applications include as coatings of bone implants [5], as porous scaffolds for bone growth [6] and as powders in bone-grafting surgery [7].

Synthesis of HAP is well known by various methods such as hydrothermal [8], mechanochemical [9], electro-spinning [10], chemical precipitation [11] and solution combustion methods [12]. Generally, the solution combustion process is based on an exothermic reaction of metal nitrates with fuel at low temperature. Numerous studies have been used to prepare ceramic oxide materials by employing solution combustion synthesis [10-13].

Recently, there has been a growing interest in synthesizing ceramic materials by self-propagating combustion synthesis (SPCS) and microwave-assisted synthesis [13-14]. It has been reported that sub-micrometre sized hydroxyapatite could be synthesized by SPCS using urea as the fuel and nitric acid as oxidizer [15]. The success of the process is due to an intimate blending among the constituents using a suitable fuel which also acts as a complexing agent (e.g., citric acid, urea, sucrose, etc.) in an aqueous medium and a vigorous exothermic redox reaction between the fuel and an oxidizer (i.e., nitric acid) [16].

To complete the combustion reaction, microwave heating can be more advantageous than conventional heating because of the short processing time and volumetric heating [17]. Microwaves are electromagnetic waves that have a frequency range of 0.3 to 300 GHz and corresponding wavelengths ranging from 1 m to 1 mm. A typical frequency for a material process is 2.45 GHz. It has long been established that dielectric materials, such as many types of ceramics can be heated with energy in the form of microwaves [18].

In this study, HAP powders were synthesized from calcium nitrate tetra hydrate and sodium phosphate dibasic

*Corresponding author:
Tel : +98-21-22952272
Fax: +98-21-22947537
E-mail: rasouli@icrc.ac.ir

anhydrous using a microwave-assisted combustion method. The formation of HAp depending on the fuel type was investigated.

## Experimental

$Ca(NO_3)_2{\cdot}4H_2O$ (0.1M, 99% pure, MERK) and $Na_2HPO_4$ were used as starting materials and glycine, citric acid and urea as fuels. The stoichiometric equations for the reaction of the three fuels with $Ca(NO_3)_2{\cdot}4H_2O$ and $Na_2HPO_4$ are given below:

$$10ca(NO_3)_2{\cdot}4H_2O + 6(NH_4)_2HPO_4 + 20C_2H_5NO_2 \rightarrow Ca_{10}(PO_4)_6(OH)_2 + 116H_2O + 40CO_2 + 20N_2 \quad (1)$$

$$10ca(NO_3)_2{\cdot}4H_2O + 6(NH_4)_2HPO_4 + 20CO(NH_2)_2 \rightarrow Ca_{10}(PO_4)_6(OH)_2 + 106H_2O + 20CO_2 + N_2 \quad (2)$$

$$10ca(NO_3)_2{\cdot}4H_2O + 6(NH_4)_2HPO_4 + 10C_6H_8O_7 \rightarrow Ca_{10}(PO_4)_6(OH)_2 + 116H_2O + 60CO_2 + 16N_2 \quad (3)$$

Stochiometric amounts of the raw materials and fuel were dissolved in 20 ml demineralized water at room temperature.

At first, fuel and calcium nitrate were taken in an uncovered glass beaker and stirred with a magnetic stirrer for 5 minuts at room temperature. The solution was acidic which was adjusted to pH 9.5 using $NH_4OH$. Then sodium phosphate dibasic anhydrous was added dropwise to the mixture under stirred conditioned and formed a gelatinous white precipitate. The pH of the solution was adjusted to 1.5 by adding concentrated nitric acid resulting in a clear solution. When the temperature was raised to 70 °C the solution became highly viscous. The mixture was reacted in a microwave oven and irradiated for 60 seconds at 900 W. Then the resultant powders were thermally treated at 900 °C for 2 h in a chamber furnace. The samples obtained in the presence of glycine, urea and citric acid were named G, U and C, respectively.

The crystal phases were characterized by X-ray diffraction (XRD, pw1800, PHILIPS company), using Cu Kα radiation (λ = 0.15418 nm). The XRD data were collected at room temperature over the 2θ range of 20-45° at a step size of 0.02°/s and a count time of 0.06 s/step. The chemical composition of the powders were analyzed by Fourier transform infrared spectroscopy (FTIR, spectrum, Perkin Elmer Ltd). The morphology of the products was studied by scanning electron microscopy (SEM, 1455vp, LEO Ltd) and a transmission electron microscope (TEM, EM 208S, PHILIPS Ltd).

## Results and Discussion

### Structural studies

The first step in the evaluation of the samples synthesized was structural studies. XRD patterns of the samples synthesized via the solution combustion method are illustrated in Figs. 1(a)-(b)-(c). As shown in figures, the hydroxyapatite structure (JCPDS No. 09-0432) appears in all samples intensely. However, a change of the fuel type affects the formation of the residual calcium oxide phase (JCPDS No.001-1160). In fact, the energy of the combustion reaction released in the G sample which consists of amine groups. On the other hand, decomposition of the mentioned groups at a lower temperature causes the creation of enough energy which leads to the formation of a pure hydroxyapatite phase. Li *et al*. [19] illustrated this phenomenon in the case of synthesis of the γ-lithium aluminate using various fuels.

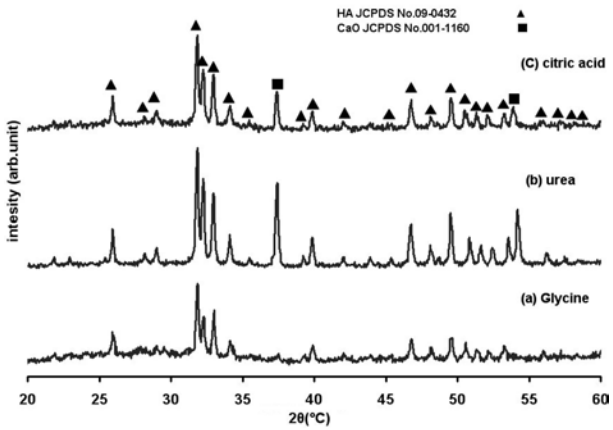


**Fig. 1.** XRD patterns of the samples synthesized via solution combustion method and three fuels.

The most important advantage of a combustion reaction is the nanocrystalline nature of products. The average crystallite size (D) was determined by Debye-Scherrer's formula according to the equation:

$$D = \frac{0.9\lambda}{B\cos\theta} \quad (4)$$

where λ is the wavelength of the incident X-rays, β is the half width of the diffracted peak and θ the is diffracted angle the values Determined of the average of the crystallite sizes versus fuel type are shown in Fig. 2. In

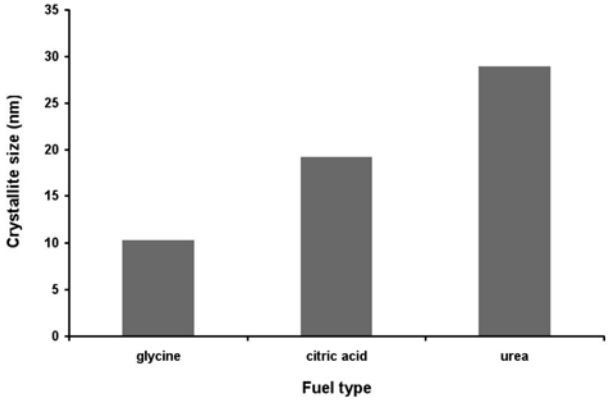


**Fig. 2.** Average crystallite size versus fuel type.

the G sample, a broadening of the XRD pattern in Fig. 1 and a decrease of the average of crystallite size in Fig. 2 confirm the effective role of the energy released on the formation of a smaller crystallite size.

## Chemical compositions

The chemical composition of powder samples has been investigated by FTIR spectroscopy. All IR spectra in this study were carefully compared with those reported earlier [20-21]. The FTIR spectra of all the samples (Fig. 3) show the characteristic peaks corresponding to $OH^-$ (625-635 $cm^{-1}$ and 3440-3640 $cm^{-1}$ ) and $PO_4^{-3}$ (565-600 $cm^{-1}$, 1045 $cm^{-1}$) vibrations, together with the weak bands of $CO_3^{-2}$ group (875-882 $cm^{-1}$ and 1420-1430 $cm^{-1}$). Carbonate can substitute in $Ca_{10}(OH)_2(PO_4)_6$ on two possible sites [21] which are distinguished by FT-IR spectroscopy. Our results indicate that the samples are carbonate substituted hydroxyapatite. Intense peaks at 877 and 1426 $cm^{-1}$ indicate the substitution of carbonate ions in the phosphate site Bs. Intense peaks at 3440-3640 $cm^{-1}$ and an absence of a peak at 1550 $cm^{-1}$ indicate that there is no carbonate substitution in OH site As.

## Morphological studies

The effect of the fuel type of the combustion reaction on the morphology of synthesized samples is illustrated in Fig. 4. As mentioned above, the G sample contains the smallest crystallite size. The morphology of this sample is shown in Fig. 4(a). A longe amount of exhaust gases leads to scattering of the irregular sub 10 nm particles to form loose agglomeration morphologies. So, morphological results are in good agreement with Sherrer's determination. Moreover, the U sample is formed of larger elongated particles which are sintered together to make a twin-like morphology (Fig. 4(b)). the XRD pattern of the U sample consists of relatively higher intensity peaks which confirms the formation of a larger particle size. However, citric acid shows a different role in the formation of particles during the combustion reaction (Fig. 4(c)). Although, fuels containing amine

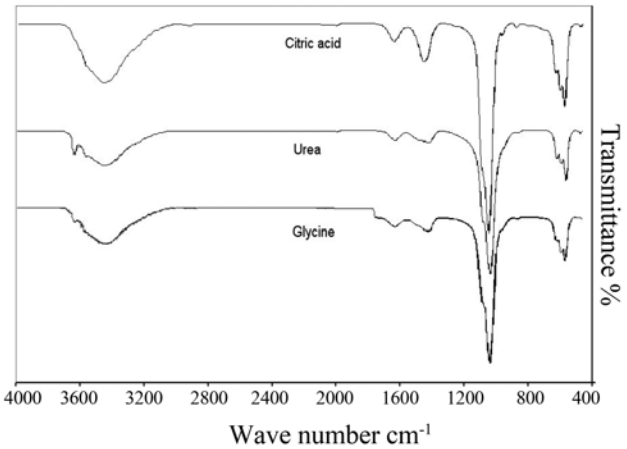


**Fig. 3.** FTIR spectra of the samples synthesized by the three fuels.

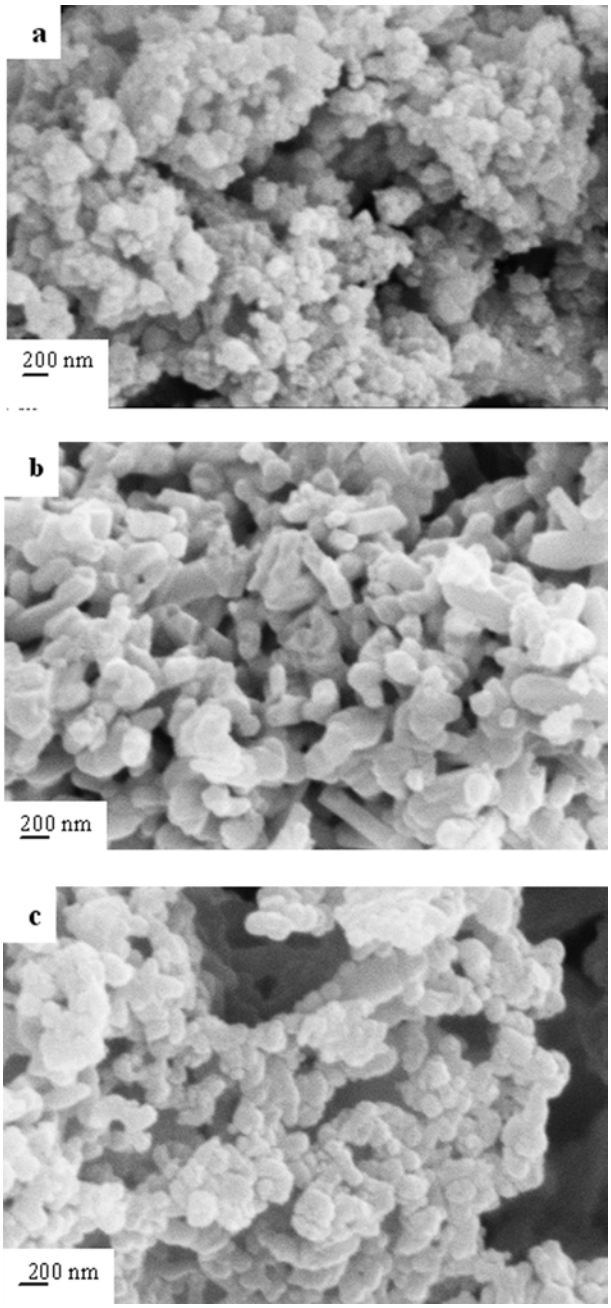


**Fig. 4.** SEM images of the samples prepared by the three fuels a) G sample, b) U sample, c) C sample.

groups decompose at a lower temperature which accelerates the combustion ignition, the citric acid fuel creates complex forms with a metal nitrate compound. These complexes during the combustion reaction induce the special features of the morphology. In C sample consists of semispherical agglomerated particles. The form and shape of the primary particles are intensely changed in the C sample. This morphology is due to the inherent effect of the organic fuel [22]. Citric acid has a more effective complexing role than glycine, because of a chelating effect [23]. Subsequently, localization of heat on the particle boundaries results in semi-sintered particles and the powder synthesized in the presence of citric

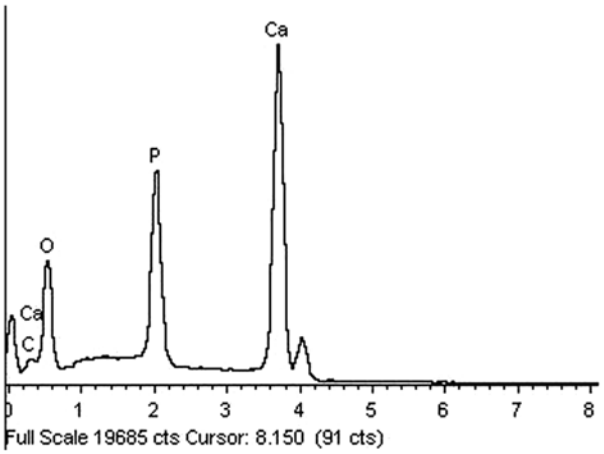


**Fig. 5.** The elemental distribution of HAP, prepared with glycine as the fuel, determined with EDX analysis.

acid has a uniform size.

The elemental distribution of HAP (prepared with glycine as the fuel) was determined with EDX analysis and is shown in Fig. 5. From Fig. 5, the EDX spectrum shows only the presence of Ca, P and oxygen. Moreover, the atomic percent age of Ca and P in the synthesized powder is about 22.76 and 10.29%, respectively. This ratio is in good agreement with the hydroxyapatite composition.

Determination of the primary particle size and morphology of G, U and C samples have been studied using TEM. Combustion in the presence of glycine led to the formation of fine rod-like nanoparticles (Fig. 6(a)) with a particle size up to 50 nm. As shown in Figs. 6(b) and (c), the particle size increased up to 100 and 200 nm in C and U samples, respectively. It seems that the primary particles in the C samples are more uniform which can be related to the carboxylic groups of citric acid. Yang *et al.* [24] showed that adsorption of growth units on crystal surfaces strongly affects the growth speed and the orientation of crystals. Hence, adsorption of the citric acid carboxylic groups on the crystal surfaces can influence the orientation and morphology of the particles [25].

In the U sample, the growth units would tend to face-land onto the growing interface. Therefore, a different growth rate of crystal planes causes twin-like morphology growth of the HAP structure [26].

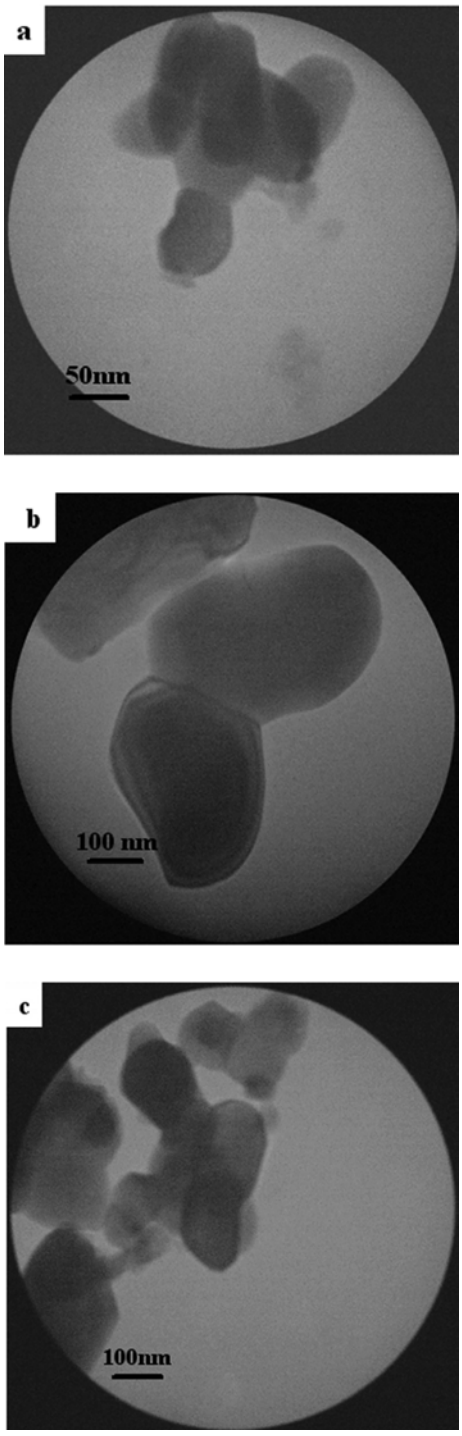


**Fig. 6.** TEM images of the samples prepared by the three fuels, a) G sample, b) C sample, c) U sample.

## Conclusions

In this study, hydroxyapatite nanopowders were successfully synthesized by using microwave irradiation via a combustion method. Results revealed that a pure hydroxyapatite phase can be obtained in the presence of glycine as the fuel. However, in the case of citric acid and urea as fuel as residual amounts of CaO were observed. Morphological studies demonstrated that the particle size and morphology are strongly dependent on the fuel type. All results confirm that finer and smaller hydoxyapatite particles can be formed by a one-step combustion process in the presence of glycine as the fuel.

## References

1. K.J.L. Burg, S. Porter and J.F. Kellam, *Biomaterials*, 21 (2000) 2347-2359.

2. L.C. Clapham, R.J.C. Mcleam and J.C. Nickel, J. Downey, J. Cryst.Growth 104 (1990) 475-484.
3. R.K. Roeder, G.L. Converse, H. Leng and W. Yue, J. Am. Ceram. Soc. 89 (2006) 2096-2104.
4. S.J. Kalita, A. Bhardwaj and H.A. Bhatt, Materials Science and Engineering: C 27 (2007) 441.
5. A. Montenero, G. Gnappi, et al., J. Mater. Sci. 35 (2000) 2719-2797.
6. J.T. Tian and J.M. Tian, J. Mater. Sci. 36 (2001) 3061-3066.
7. H. Oonishi, L.L. Hench, et al., J. Biomed. Mater. Res. 44 (1999) 31-43.
8. K. Lin, J. Chang, R. Cheng and M. Ruan, Mater. Lett. 61 (2007) 1683-1687.
9. C. Shu, W. Yanwei, L. Hong, P. Zhengzheng and Y. Kangde, Ceram. Int. 31 (2005) 135-138.
10. Y. Wu, L.L. Hench, J. Du and K.L. Choy, J. Guo, J. Am. Ceram. Soc. 87 (2004) 1988-1991.
11. Y. Liu, W. Wang, Y. Zhan, C. Zheng and G. Wang, Mater. Lett. 56 (2002) 496-501.
12. A.L. Macipe, J.G. Morales and R.R. Clemente, Adv. Mater. 10 (1998) 49-53.
13. S. Sasikumar and R. Vijayaraghavan, Trends Biomater. Artif. Organs 19[2] (2006) 70-73.
14. B. Vaidhyanathan and K.J. Rao, Bull. Mater. Sci. 19 (1996) 1163-1165.
15. A. Cuneyt Tas, J. Eur. Ceram. Soc. 20 (2000) 2389-2394.
16. R.Z. LeGeros, O.R. Trautz, J.P. LeGeros, E. Klein and W. Paul Sirra, Science 158 (1967) 1409-1411.
17. A. Lagashetty, V. Havanoor, S. Basavaraja, S.D. Balaji and A. Venkataraman, Science and Technology of Advanced Materials, 8 [6] (2007), 484-493.
18. D.E. Clark, I. Ahmad and R.C. Dalton, Materials Science and Engineering: A, 144 (1991) 91-97.
19. F.i Li, K. Hu, J. Li, D. Zhang and G. Chen, J. Nuclear Materials, 300[1] (2002) 82-88.
20. F. Miyaji, Y. Kono and Y. Suyama, Mater. Res. Bull. 40 (2005) 209-220.
21. D.K. Pattanayak, R. Dash, R.C. Prasad, B.T. Rao and T.R. Rama Mohan, Materials Science and Engineering: C 27 (2007) 684-690.
22. R.V. Mangalaraja, J. Mouzon, P. Hedström, Carlos P. Camurri, S. Ananthakumar and M. Odén, Powder. Technol. 191 (2009) 309-314.
23. K.H. Wu, T.H. Ting, M.C. Li and W.D. Ho, J. Magnet. Magnet. Mater. 298 (2006) 25-32.
24. Z.Yang, Q-H. Liu and L.Yang, Mater. Res. Bull. 42 (2007) 221-227.
25. Y. Liu, C-y.Liu and Z-y.Zhang, Chem. Eng. J. 138 (2008) 596-601.
26. S.K. Sharma, S.S. Pitale, M.M. Malik, R.N. Dubey, M.S. Qureshi and S. Ojha, Physica B: Condensed Matter, 405[3] (2010) 866-874.